THE JOURNAL OF BIOLOGICAL CHEMISTRY
Vol. 278, No. 42, Issue of October 17, pp. 40959–40966, 2003

Printed in U.S.A.

The Staphostatin-Staphopain Complex

A FORWARD BINDING INHIBITOR IN COMPLEX WITH ITS TARGET CYSTEINE PROTEASE*

Received for publication, March 21, 2003, and in revised form, July 8, 2003
Published, JBC Papers in Press, July 21, 2003, DOI 10.1074/jbc.M302926200

Renata Filipek‡§¶‖, Malgorzata Rzychon‡§¶‖, Aneta Oleksy¶, Milosz Gruca¶, Adam Dubin¶, Jan Potempa¶, and Matthias Bochtler‡§‡‡**

*From the ‡International Institute of Molecular and Cell Biology, ul. Trojdena 4, 02-109 Warsaw, Poland, the §Max-Planck-Institute for Molecular Cell Biology and Genetics, Pfotenhauerstr. 108, 01309 Dresden, Germany, the ¶Faculty of Biotechnology, Jagiellonian University, Gronostajowa 7, 30-387 Kraków, Poland, and the **Department of Biochemistry and Molecular Biology, University of Georgia, Athens, Georgia 30602*

Staphostatins are the endogenous inhibitors of the major secreted cysteine proteases of *Staphylococcus aureus*, the staphopains. Our recent crystal structure of staphostatin B has shown that this inhibitor forms a mixed, eight-stranded β-barrel with statistically significant similarity to lipocalins, but not to cystatins. We now present the 1.8-Å crystal structure of staphostatin B in complex with an inactive mutant of its target protease. The complex is held together through extensive interactions and buries a total surface area of 2300 Å². Unexpectedly for a cysteine protease inhibitor, staphostatin B binds to staphopain B in an almost substrate-like manner. The inhibitor polypeptide chain runs through the protease active site cleft in the forward direction, with residues IG-TS in P2 to P2′ positions. Both in the free and complexed forms, the P1 glycine residue of the inhibitor is in a main chain conformation only accessible to glycines. Mutations in this residue lead to a loss of affinity of the inhibitor for protease and convert the inhibitor into a substrate.

The emergence of multiple antibiotic resistance in Staphylococci, in particular *Staphylococcus aureus*, has become a major medical concern. With the prevalence of methicillin-resistant *S. aureus* in hospitals throughout the world (1, 2) and with the appearance of strains that are resistant to "last resort" glycopeptide antibiotics (3, 4), treatment of *S. aureus* infections in difficult cases could soon depend on a few new compounds that have either been recently introduced to the clinic or are still in clinical trials (5–9). A possible strategy for the development of new antibacterials is to target bacterial virulence factors. The *S. aureus* arsenal of virulence factors includes secreted toxins (10, 11), immune modulatory molecules (12), adhesion molecules (13), signaling factors (14, 15), and possibly secreted proteases (16).

Staphopains A and B are the major secreted cysteine proteases of *S. aureus*. The literature contains evidence both for and against their role as virulence factors. Random mutagenesis has shown that transposon insertion into the V8-proteinase gene attenuates *S. aureus* virulence in three separate animal models (mouse abscess, bacteraemia, and wound infection models) (17). More recent work suggests that loss of virulence could be because of a polar effect of the insertion event on the downstream *sspB* gene encoding staphopain B (18). Consistent with this, inactivation of the *sspB* gene attenuates *S. aureus* virulence in the skin abscess model. In contrast, staphopain A, a close homologue of staphopain B, appears to be dispensable for virulence at least in this model.[1]

Staphopains A and B are remote members of the papain superfamily of enzymes and are encoded on the genome as preproenzymes in the *scp* and *ssp* loci, respectively. Recently, it was shown that a short open reading frame in the *ssp* operon termed *sspC* codes for an inhibitor of staphopain B, the cysteine protease in this operon (19). This initial finding could be extended to the *scp* operon: the second open reading frame in this operon, termed *scp*B, codes for an inhibitor of ScpA/staphopain A (20). Despite the homology between staphopains A and B (47% amino acid identity over 174 residues) and between the *scp*B and *ssp*C gene products (18% amino acid identity over 109 residues), the inhibitors are specific for the proteases in their own operon. To emphasize this extraordinary specificity against the staphylococcal proteases and other papain-like proteases, they have been termed staphostatin A and B, respectively (20).

The structure of mature staphopain A is known (21). It shows that staphopains are remote members of the papain superfamily of enzymes with cathepsin B as their closest structural neighbor among the eukaryotic enzymes. Our recent determination of the staphostatin B structure (22) has shown that staphostatins are not significantly similar to cystatins at the structural level, even though they resemble type I and II cystatins in length and secondary structure. Staphostatins form eight-stranded mixed β-barrels, which result from hydrogen bonding of a three-stranded ψ-loop motif to a five-stranded, antiparallel β-sheet on both sides. In structural terms, staphostatin B is most closely related to lipocalins and to a number of protease inhibitory and regulatory domains that form β-barrels. In this article, we present the crystal structure of the staphostatin B-staphopain B complex at 1.8-Å resolution and report evidence that the unusual binding mode is relevant in solution as well.

* This work was supported by the Commission of the European Communities, specific RTD program "Quality of Life and Management of Living Resources," QLRT-2001-01250, "Novel non-antibiotic treatment of staphylococcal diseases," and Committee for Scientific Investigation (KBN) Grants 6P04A08320, 1789/E-529/SPB/5.PR UE/DZ 600/2002-2005, and 158/E-338/SPB/5.PR UE/DZ 19/2003. The costs of publication of this article were defrayed in part by the payment of page charges. This article must therefore be hereby marked "*advertisement*" in accordance with 18 U.S.C. Section 1734 solely to indicate this fact.

The atomic coordinates and structure factors (code 1PXV) have been deposited in the Protein Data Bank, Research Collaboratory for Structural Bioinformatics, Rutgers University, New Brunswick, NJ (http://www.rcsb.org/).

‖ Both authors contributed equally to the results of this work.

‡‡ To whom correspondence should be addressed. Tel.: 48-22-6685193; Fax: 48-22-6685288; E-mail: MBochtler@iimcb.gov.pl.

[1] L. Shaw, E. Golonka, J. Potempa, and S. Foster, submitted for publication.

EXPERIMENTAL PROCEDURES

Cloning, Expression, and Protein Purification—Staphostatin B was recombinantly expressed in *Escherichia coli* and purified as described before (20). Mutants of staphostatin B were generated according to the QuikChange (Stratagene) site-directed mutagenesis protocol and could be purified like the wild-type with the exception of the C-terminal deletion mutant (Δ99–109) that was insoluble.

For purification of staphopain B from the native source, culture supernatant was brought to 80% ammonium sulfate saturation. Precipitated proteins were collected by centrifugation (10,000 rpm, 30 min) and the pellet was dissolved in 50 mM Tris, pH 7.6. After extensive dialysis against the same buffer, the sample was clarified by centrifugation (10,000 rpm, 1 h) and loaded on a DE-52 column (Whatman) pre-equilibrated with 50 mM Tris, pH 7.6. After extensive washing, bound protein was eluted with a NaCl gradient (0–500 mM). Elution fractions were checked by SDS-PAGE and assayed for proteolytic activity by zymography or by the azocoll (Calbiochem) assay (23). Fractions containing staphopain B (typically 70–100 mM NaCl) were pooled, dialyzed against 50 mM sodium phosphate buffer, pH 7.0, supplemented with 2 M ammonium sulfate, and subjected to hydrophobic chromatography on phenyl-Sepharose (Amersham Biosciences). In a final step, the eluate was dialyzed against 50 mM Tris, pH 7.6, to remove salt.

Alternatively, prostaphopain B was cloned into pGEX-5T (24) and expressed in *E. coli* as a glutathione *S*-transferase fusion construct with the N-terminal glutathione *S*-transferase moiety linked to proenzyme via a thrombin cleavable linker. The hybrid protein was purified by affinity chromatography on glutathione-Sepharose 4B (Amersham Biosciences) and cleaved on the column with V8 protease at room temperature (5 h, 1:1000 weight ratio of the V8 proteinase to prostaphopain B). Eluted protein was then bound to thiopropyl-Sepharose 6B (Amersham Biosciences) and washed with 200 mM NaCl in 100 mM Tris, pH 7.8. Staphopain B was recovered from the column with 20 mM dithiothreitol in 50 mM Tris, pH 8.0. In some purifications, this affinity purification step was replaced with hydrophobic chromatography on phenyl-Sepharose (Amersham Biosciences) running a gradient from 2 to 0 M ammonium sulfate in 50 mM Tris, pH 7.5. The protein eluted close to the end of the gradient.

Both procedures yielded sufficient amounts of enzyme for analytical work, but not enough protein for crystallization. Therefore, we settled for an inactive mutant of mature staphopain B with alanine replacing the active site cysteine. A variant of overlap PCR was used to generate the mutant open reading frame, which was subsequently cloned via *Eco*RI and *Xho*I into a derivative of pET15b (Novagen) that lacks the original *Eco*RI site of the vector and carries six histidines and an *Eco*RI site downstream of the original *Nco*I site. Thus, the N-terminal sequence of our construct was MGHHHHHHEFDQV . . . , where DQV are the first residues of the native staphopain B sequence. *E. coli* BL21(DE3) were grown at 37 °C and, after induction with 0.5 mM isopropyl-1-thio-β-D-galactopyranoside, were shifted to 30 °C for 5 h.

Cells were harvested, resuspended in 5 mM Tris, pH 7.5, with lysozyme and DNase I, and opened by sonication as usual. After centrifugation (40,000 rpm, 30 min) to remove insoluble debris, supernatant was applied to a nickel-nitrilotriacetic acid-agarose (Qiagen) column. The column was washed with 10 mM imidazole in buffer A (20 mM Tris, pH 7.5, 50 mM NaCl) and eluted with 30 mM imidazole also in buffer A. The eluate was concentrated, mixed with a slight stoichiometric excess of inhibitor, and the mixture applied to a Sephacryl S-300 (Amersham Biosciences) gel filtration column in buffer B (5 mM Tris, pH 7.5, 1 mM EDTA). The eluate was concentrated on YM-10 Centricons to a final OD (280 nm) between 30 and 50 and used for crystallization.

Analysis of Inhibitor Processing—Inhibitor processing was tested with protease preparations from both recombinant and native sources. Incubation with the protease was done in 5 mM Tris, pH 7.4, and in the presence of 2 mM cysteine to maintain the activity of staphopain B. For MALDI-TOF[2] traces, incubations were done at room temperature, and recombinant protease was used in 1:1 molar ratio with inhibitor. Mass spectrometry analysis was performed with a Bruker Reflex IV MALDI-TOF spectrometer equipped with delayed ion extraction working in the linear mode. All samples were prepared by the dried droplet method. Briefly, 0.5 μl of sample was mixed with an equal volume of matrix solution (saturated solution of sinapinic acid in 96% ethanol) and 0.5 μl of the mixture was deposited on a stainless steel target plate.

Design and Characterization of a Synthetic Staphopain B Substrate—The fluorescence-quenched peptide Abz-Gln-Gly-Ile-Gly-Thr-Ser-Arg-Pro-Lys(Dnp)-Asp-OH was designed as a mimic of the binding loop of staphopain B and was synthesized by Auspep Pty. Ltd. (Parkville, Australia). Mass spectrometry confirmed that staphopain B cleaves the substrate into fragments Abz-Gln-Gly-Ile-Gly-OH and H_2N-Thr-Ser-Arg-Pro-Lys(Dnp)-Asp-OH, as expected from the staphostatin B-staphopain B cocrystal structure. Substrate hydrolysis was monitored with a Shimadzu spectrofluorophotometer (model RF-5301 PC) with λ_{ex} = 325 nm and λ_{em} = 414 nm. All assays to characterize the substrate were done in 50 mM Tris-HCl, pH 7.4, containing 2 mM cysteine, 0.001% (w/v) CHAPS, and 5 mM EDTA. The dissociation constant K_m was estimated from the dependence of the initial velocity of the reaction on substrate concentration (between 10 and 60 μM) by hyperbolic regression analysis (program Hyper, version 1.1s, 1996). The estimate of K_m was ~38 μM.

For the determination of k_{cat}/K_m, staphopain B (50, 100, 150, 200, and 250 nM) was added to 1 μM substrate and the fluorescence intensity (INT) was followed for 30 min (data not shown). Progress curves were fitted to the equation $INT = I_o + I_{max}(1\text{-}\exp(-[E]\,k_{cat}/K_m\,t))$, where I_o is the initial fluorescence of the uncleaved substrate, I_{max} the maximum fluorescence intensity, and $[E]$ is the total enzyme concentration, which describes the expected change of fluorescence over time for $[S] \ll K_m$. The k_{cat} was found to be 1.7 s^{-1} for our buffer conditions.

Analysis of Inhibitor Affinity—Analytical gel filtration runs were performed with a Superose 12 HR 10/30 (Amersham Biosciences) column in buffer C (50 mM sodium phosphate, pH 7.0, 150 mM NaCl). Quantitative assays of protease inhibitor dissociation constants were done with the synthetic substrate Abz-Gln-Gly-Ile-Gly-Thr-Ser-Arg-Pro-Lys(Dnp)-Asp-OH in 50 mM Tris, pH 7.4, 5 mM EDTA, 2 mM cysteine. Assays were done in a 600-μl reaction volume with either 50 or 100 nM staphopain B and 1 μM substrate. Initial hydrolysis rate was determined as a function of inhibitor concentration (varied between 0 and 100 μM inhibitor). The ratio of v_o/v of the initial velocity in the absence of inhibitor *versus* the initial velocity in the presence of the inhibitor is expected to depend on the apparent K_i^* according to $v_o/v = 1 + [I]/K_i^*$, where K_i^* is the apparent inhibitor dissociation constant and $[I]$ the inhibitor concentration. Apparent inhibitor affinities K_i^* were read from Dixon-type plots, and were essentially identical to true affinities for K_i as expected from the equation $K_i^* = (1 + [S]/K_m)K_i$ and as demonstrated experimentally by a variation of substrate concentration (from 1 to 10 μM). The K_i determination would have profited from measurements at higher inhibitor concentrations for the G98R variant. Because of limited solubility of the mutant, this was unfortunately not possible.

Crystallization—Initial crystallization screens were set up at room temperature (21 °C) using the vapor diffusion method in sitting drops with 0.5 ml of reservoir and a mixture of 2 μl of reservoir and protein solution each in the crystallization drop. With a reservoir solution containing 2 M $(NH_4)_2SO_4$ and 5% isopropyl alcohol, initial, but intergrown crystals could be obtained. This problem was overcome with the addition of 0.4 μl of 1.0 M guanidine hydrochloride. Crystals could be grown over a period of between 1 and 2 weeks, but deteriorated within fractions of a minute upon opening the crystallization container, even without any addition of reservoir buffer. After much experimentation, we learned that after injecting buffer D (a 9:1 mixture of 2.8 M $(NH_4)_2SO_4$ and (2*R*,3*R*)-(−)-2,3-butanediol) into the drop, the container could be opened safely and the crystal transferred to buffer D, which was sufficient for cryoprotection. The best specimen frozen in this way diffracted on BW6/DESY to 1.8 Å. Crystals contained two copies of the protease and the inhibitor each in the asymmetric unit and belonged to space group P212121. Detailed characteristics of our synchrotron dataset are presented in Table I.

Structure Determination—Structure solution was greatly aided by the availability of the structure of mature staphopain A (21) that allowed us to construct a homology model for staphopain B with all non-conserved side chains mutated to alanine using SCWRL (25). With this search model, an automated MOLREP (26) run searching for two copies of our homology model identified a clear solution. Further MOLREP searches for the inhibitor molecules were unsuccessful, but FFFEAR (27) searches in maps generated with phases from the two placed protease molecules correctly located one of the two inhibitor molecules, which could easily be associated with a particular copy of the protease in our crystals. Application of the local symmetry between the two copies of protease in the asymmetric unit then identified the second copy of inhibitor. At the time the structure was solved the high resolution synchrotron dataset was not available. Once this dataset became available, we repeated the structure solution starting from the two

[2] The abbreviations used are: MALDI-TOF, matrix-assisted laser desorption ionization time-of-flight; Abz, *o*-aminobenzoyl; CHAPS, 3-[(3-cholamidopropyl)dimethylammonio]propanesulfonic acid; Dnp, 2,4-dinitrophenyl; ssp, staphylococcal serine protease.

TABLE I
Data collection and refinement statistics

Data collection statistics	
Space group	P212121
a (Å)	73.49
b (Å)	94.97
c (Å)	110.93
Independent reflections	64,796
Resolution (Å)	1.8
Completeness (%)	92%
R_{sym} (%) (last shell in brackets)	5.2 (18.2)
I/σ (last shell in brackets)	9.8 (3.5)
Refinement statistics	
R-factor (%)	19.2
R_{free}	22.1
Root mean square deviation bond distance (Å)	0.02
Root mean square deviation angles (°)	2
Ramachandran core (%)	88.6
Ramachandran additionally all (%)	11.0
Ramachandran generously all (%)	0.4
Ramachandran disallowed (%)	0

placed copies of protease. Automatic ARP/WARP (28) model building produced a largely complete main chain trace for both copies of inhibitor in the asymmetric unit, thus providing another independent conformation for the staphostatin B fold. Data collection and refinement parameters are presented in Table I.

RESULTS

Expression, Purification, Crystallization, and Structure Determination—Staphostatin B was expressed and purified as previously described (20). Several attempts to heterologously express recombinant mature staphopain B in *E. coli* failed, presumably because of toxicity of the active protein to its host. We therefore settled for an inactive mutant of the protease with alanine replacing the active site cysteine. This inactive form of staphopain B could be expressed in *E. coli* in quantity, and a version with the N-terminal His tag could be purified in good yield (see "Experimental Procedures"). Gratifyingly, comigration of inactive protease and inhibitor both in native gels and on gel filtration columns confirmed that the mutant form of the protease had retained the strong affinity of the wild-type for its inhibitor.

We thus proceeded to crystallize the complex from stoichiometric mixtures of protease and inhibitor. Crystals diffracted to 1.8 Å on BW6/DESY. The structure was easily solved with models of the components as described under "Experimental Procedures." Briefly, we used molecular replacement to locate two copies of the homology model of staphopain B that were based on the published structure of mature staphopain A (21). Maps phased with this partial model were of sufficient quality to locate the two copies of inhibitor in two independent ways. The extent of protein-protein contacts leaves no doubts as to which inhibitor molecule should be assigned to which protease molecule. Although located in different environments, the two complexes in the asymmetric unit are essentially identical. A summary of data collection and refinement parameters is presented in Table I.

The Structure of Staphopain B—As expected from the high sequence identity between staphopains A and B, the structure of staphopain B is in excellent agreement with the homology model that could be produced on the basis of the staphopain A structure (21). Briefly, like all proteases that belong to the papain clan of cysteine proteases, staphopain B consists of two domains, which are generally referred to as the L- and R-domain according to their orientation left and right of the active site cleft in the "standard view" for this superfamily of proteases (29) (see Fig. 1).

As in other superfamily members, the L-domain is built from the N-terminal part of the sequence with the exception of the most N-terminal residues, and contains the active site helix that carries the nucleophilic cysteine at its amino terminus. In staphopains, the L-domain is more compact than in other papain-like enzymes. In essence, it only contains one additional helix and the linker that connects it to the R-domain.

The R-domain contributes the catalytic histidine and asparagine and is built around a six-stranded, antiparallel pseudobarrel. We consider the barrel "pseudo," because the two strands formed from residues Ser-367 to Asp-370 and from residues Leu-375 to Leu-378 are too far apart to be linked by main chain hydrogen bonds. The barrel is significantly different from the barrel in all other papain-like proteases, including cathepsin B, by far the closest staphopain relative (see Fig. 1). One hairpin that contributes two strands to the staphopain barrel is so far unique to staphopains, and a second hairpin loop is significantly shorter and does not bend backwards as in all other papain-like enzymes.

The Staphostatin B-Staphopain B Interface—In standard orientation staphostatin B binds to the "top" of staphopain (see Fig. 2*A*), roughly interacting with the analogous segments of protease that are also used for contacts with either cystatins (30) (see Fig. 2*B*) or the globular domains of profragments (31, 32) (not shown). Nevertheless, because the staphostatin, cystatin, and profragment folds are unrelated, the details of the staphostatin B-staphopain B interaction are without precedence in protease-inhibitor complexes so far. The interaction of staphopain B with staphostatin B buries a total surface area of about 2300 $Å^2$ and involves contacts of the inhibitor with the L- and R-domains and the active site cleft of protease.

Excluding contacts of the active site spanning residues with protease, there are few specific contacts of the inhibitor with the L-domain. An array of ordered water molecules is located at the interface between protease and inhibitor in both copies of the complex in the asymmetric unit of our crystals. In at least one copy of the complex, there is some additional, as yet unidentified density possibly representing a component of the buffer, and in one copy of the complex, Asp-239 of protease forms a salt bridge with Lys-38 of inhibitor.

The R-domain of protease makes only contacts with residues in the C-terminal half of the inhibitor sequence. Once more excluding contacts to the active site spanning residues of inhibitor, all contacts are contributed by residues that are located in two loops of the six-stranded pseudobarrel of protease. Interestingly, these are the two loops that are specific for staphopains in the papain superfamily (see Fig. 2). We therefore expect that the contacts of inhibitor with R-domain contribute significantly to the specificity of staphostatins for staphopains. In particular, the salt bridge of Lys-66 of inhibitor with Asp-335 of protease and the salt bridge between Asp-80 of inhibitor and Arg-382 of protease appear favorable.

Staphostatins Bind Similar to Substrates—The most prominent interactions between staphostatin B and staphopain B are mediated through loop residues 97 to 101 of inhibitor that span the active site of protease in the forward direction (see Fig. 2*A*). In analogy to "standard mechanism" inhibitors of serine proteases, we call this loop of inhibitor "the binding loop." The binding loop is very well ordered in the staphostatin B-staphopain B complex, and its conformation is essentially identical in both copies of the complex in the asymmetric unit. Interestingly, this conformation does not appear to be preformed in free staphostatin B, because both copies of inhibitor in crystals of staphostatin B alone (22) are significantly different (see Fig. 3*A*). Although the binding loop is of course not cleaved by the inactive alanine mutant of protease in our crystals, the interaction with protease is best described in terms of

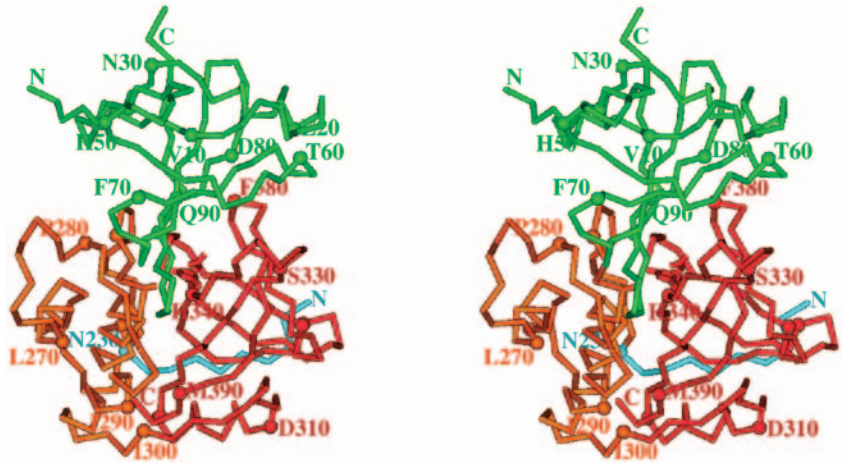

FIG. 1. **Stereo Cα trace of the staphopain B-staphostatin B complex in standard orientation for papain-like cysteine proteases.** The L- and R-domains of protease are colored *orange* and *red*, respectively, and correspond to the N- and C-terminal portion of the sequence. The very N terminus of staphopain B that defies this rule is colored in *light blue*. The inhibitor is shown in *green*. For both staphopain B and staphostatin B, every tenth residue is shown as a *ball*, and has been labeled where possible without undue crowding. Protease with chain ID *A* and inhibitor with chain ID *C* were used for the figure.

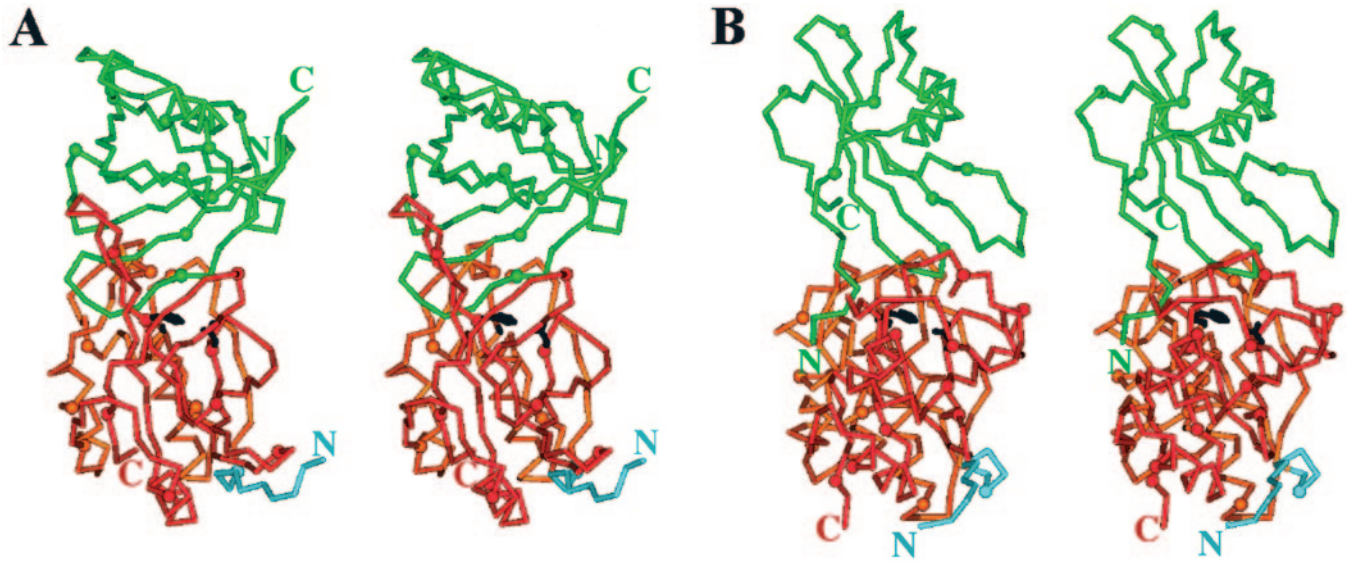

FIG. 2. **Stereo Cα traces of the staphopain B-staphostatin B complex (*A*) and of the papain-human stefin B complex (1STF) as described in Ref. 30 (*B*).** The coloring is consistent with Fig. 1, but the orientation is different. Every tenth residue is again marked with a *ball*. Protease with chain ID *A* and inhibitor with chain ID *C* were used for the figure.

Berger and Schechter's nomenclature (33) for the interaction between substrates and their target proteases.[3]

Residues P2 to P3′ of the binding loop are in contact with protease (see Fig. 3*B*). The P2 residue in staphostatin B is Ile-97. Its carbonyl oxygen and amide are engaged in hydrogen bonds with Thr-284 of protease, and the side chain inserts into a hydrophobic pocket lined by residues Pro-286, Met-289, Leu-325, Ala-341, and Tyr-387 (S2 pocket not shown in Fig. 3*B*). The isoleucine side chain does not seem to fill the pocket entirely, and leucine could fit as well. As the P2 residue in staphostatin A is leucine, we suspect that the extraordinary specificity of staphostatins for the proteases in their own operon is probably not because of S2-P2 interactions.

The P1 residue is Gly-98, a conserved glycine in all known staphostatin sequences. With Ramachandran angles $(\varphi,\psi) \sim (145°, 120°)$, this residue has a strained backbone conformation that would be sterically forbidden for any other residue (and lead to a close contact of the Cβ with Ser-241O of protease). It appears that this conformation is mainly fixed through hydrogen bonds, although in part indirectly. Gly-98NH donates a hydrogen bond to Gly-339O and may receive hydrogen bonds from either Ser-92Oγ H or Ser-93NH. Whereas the hydrogen bond to Gly-339O is convincing, atomic distances suggest that Ser-92Oγ H is more likely to donate its hydrogen bond to Thr-99Oγ, which in turn donates a hydrogen bond to Gly-339O, and the relatively long bond distance and poor geometry argue against a hydrogen bond from Ser-93NH to Gly-98O. Thus, it seems more likely that the conformation of the P1 glycine is indirectly fixed through the amide bond to the P1′ residue.

The P1′ residue Thr-99 contributes major interactions with protease. In addition to the above described interactions of its side chain O-γ, it accepts a hydrogen bond from Trp-362Nε H to its carbonyl oxygen and its main chain NH would be ideally positioned to donate a hydrogen bond to His-340Nδ, the histidine of the catalytic triad. Assignment of this hydrogen bond implies that His-340 is uncharged and in the tautomeric state with the proton on N-ε. This is unproven for the pH of our crystals (around 6.3), and unusual at least for wild-type papain-like cysteine proteases that would be expected to contain a thiolate-imidazolium ion pair in their active sites (34).

The P2′ residue Ser-100 is again fixed through hydrogen bonds, but in contrast to the P1′ residue, all its hydrogen bonding partners are residues of inhibitor and not of protease.

[3] This nomenclature describes residues of a protease substrate according to their distance to the scissile peptide bond. Residues on the N-terminal side are called P1, P2, P3, etc., with P1 closest to the scissile bond. Residues on the C-terminal side are referred to as P1′, P2′, P3′, etc. The corresponding binding sites for these residues in the protease active site cleft are called S1, S2, S3, etc., and S1′, S2′ and S3′, etc., respectively.

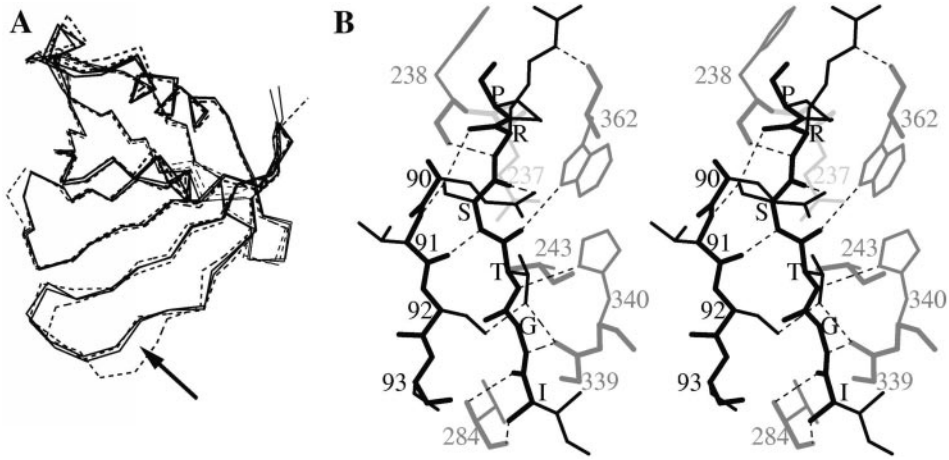

FIG. 3. *A*, superposition of the staphostatin B models in the orientation of Fig. 2*A*. *Solid lines* represent the two molecules of inhibitor in the asymmetric unit of the staphostatin B-staphopain B complex crystals (this work), and *dashed lines* show the conformations of the two molecules of inhibitor in the asymmetric unit of the staphostatin B crystals (22). The *arrow* points to the binding loop of inhibitor. The strong deviation of copy *B* of free inhibitor in this region is because of crystallographic contacts (not shown). *B*, stereo diagram of hydrogen bonds (*dashed lines*) between inhibitor (*black*) and protease (*gray*). Residues of the binding loop are labeled by residue type, all other residues are labeled by residue number. Ala-243 replaces the active site cysteine in our staphopain B mutant, and His-340 is the active site histidine of protease. Protease with chain ID *A* and inhibitor with chain ID *C* were used for the figure.

The side chain of the P3′ residue Arg-101 faces protease again, hydrogen bonds with Trp-362O, and fills a cleft lined on one side by Trp-362 and Phe-380 and on the other side by Gln-236 and Phe-238.

The staphostatin B-staphopain B binding mode results in a remarkable placement of the scissile peptide bond relative to the catalytic residues of protease. Although our crystals contain an inactive variant of protease with alanine replacing the active site cysteine, the location of the nucleophilic sulfur can be tentatively inferred from its location in the staphopain A structure (21). According to this model, it would be placed almost in the plane of the P1-P1′ peptide bond behind the carbonyl carbon so that the O-C-S angle would be close to 180°, a far too high value for efficient nucleophilic attack (35).

Mutations of the P1 Glycine of Inhibitor Reduce the Affinity for Protease—The most conspicuous feature of the binding mode of staphopain B to staphostatin B is the strained backbone conformation of the P1 glycine that would be Ramachandran forbidden for any other amino acid. To test the importance of this conformation, we generated staphostatin B mutants with alanine and arginine replacing the P1 glycine. Both mutations resulted in a loss of affinity for staphopain B. In native gel electrophoresis, only wild-type inhibitor, but neither of the inhibitor mutants comigrate with protease. This is true both for wild-type protease and for the inactive staphopain B mutant. In gel filtration experiments, the inactive mutant of protease comigrated almost quantitatively with wild-type inhibitor, partially with the alanine mutant of inhibitor, and not at all with the arginine mutant of inhibitor (see Fig. 4).

To make this observation quantitative, a synthetic substrate was needed. Based on the sequence of the binding loop in staphostatin B, we designed the synthetic quenched-fluorescence substrate Abz-Gln-Gly-Ile-Gly-Thr-Ser-Arg-Pro-Lys-(Dnp)-Asp-OH. Dissociation constant and turnover number for this substrate were determined as described under "Experimental Procedures" and found to be 38 ± 10 μM (see Fig. 5*A*) and 80 ± 10 min^{-1} (data not shown), respectively. With these parameters, the assay was too insensitive to accurately determine the high affinity between staphopain B and staphostatin B. However, the observation that 10 nM wild-type staphostatin B abolished the activity of 5 nM staphopain B within experimental error (see Fig. 5*B*) implies that the dissociation constant for the wild-type components must be lower than 10 nM. In contrast to the situation with wild-type inhibitor, the synthetic substrate was sensitive enough to characterize staphostatin B mutants. From the Dixon-type plots in Fig. 5, we infer a binding constant of 5 ± 1 μM for the G98A mutant (see Fig. 5*C*) and a binding constant greater than 100 μM for the G98R mutant (see Fig. 5*D*).

Staphostatins Can Be Cleaved between the P1 and P1′ Residue—The substrate-like binding mode of staphostatin B to staphopain B raises the possibility that the inhibitor could be cleaved by its target protease. Whereas this is of course excluded for our crystals that contain an inactive protease mutant, it could conceivably happen in solution on incubation of wild-type protease with inhibitor. To address the question of inhibitor cleavage experimentally, we purified active protease from *S. aureus* culture supernatants and through *in vitro* V8 protease-mediated cleavage of recombinantly produced prostaphopain (see "Experimental Procedures"). With both preparations of staphopain B, even prolonged incubation of protease with inhibitor led to either no degradation of inhibitor at all, or to the generation of a band that ran just slightly faster than the full-length inhibitor on denaturing SDS-PAGE gels (after boiling samples in reducing sample buffer). The time course of the generation of this band was somewhat peculiar: with protease preparations that did lead to the generation of the minor band, an initial amount of truncated inhibitor appeared very rapidly (on the subminute time scale) on mixing. No further processing was observed (data not shown).

Additional evidence indicates that the minor band on our gels represents processed staphostatin B, which has been cleaved by staphopain B exactly in the position predicted from the crystallographic studies. First, N-terminal sequencing confirmed that the N-terminal sequence of the minor band matches the sequence of the N terminus of the inhibitor. Second, and more conclusively, the predicted and experimentally determined masses for the processed inhibitor agree to within ±2 Da, well within the error margin of the MALDI-TOF setup (see Fig. 6*A*).

Mutations to the P1 Glycine Convert Staphostatins to Substrates—Interestingly, mutations in the P1 glycine of staphostatin B make the inhibitor more susceptible to proteolysis by staphopain B: incubation of the P1 alanine mutant of inhibitor with protease for 30 min yields two peaks in MALDI-TOF, one for uncleaved inhibitor and a second, very substantial peak

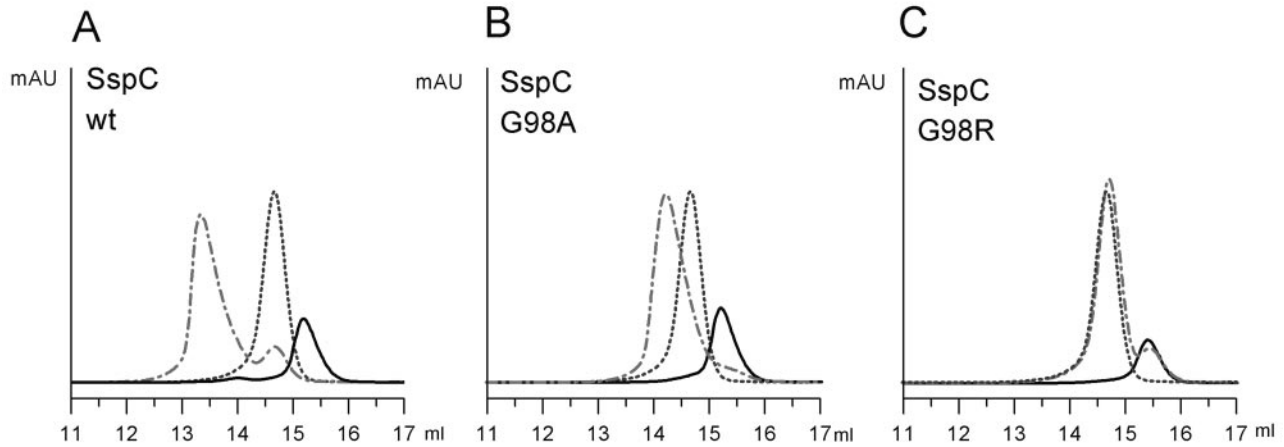

FIG. 4. **Gel filtration profiles for wild-type (*wt*) inhibitor and the P1 glycine to alanine and glycine to arginine mutants.** The *dotted trace* (*dark gray*) is obtained if only the inactive alanine mutant of protease is injected. The continuous trace (*black*) shows the result of injecting inhibitor only. The *dot-dashed trace* (*light gray*) shows the migration behavior if protease and inhibitor are coinjected.

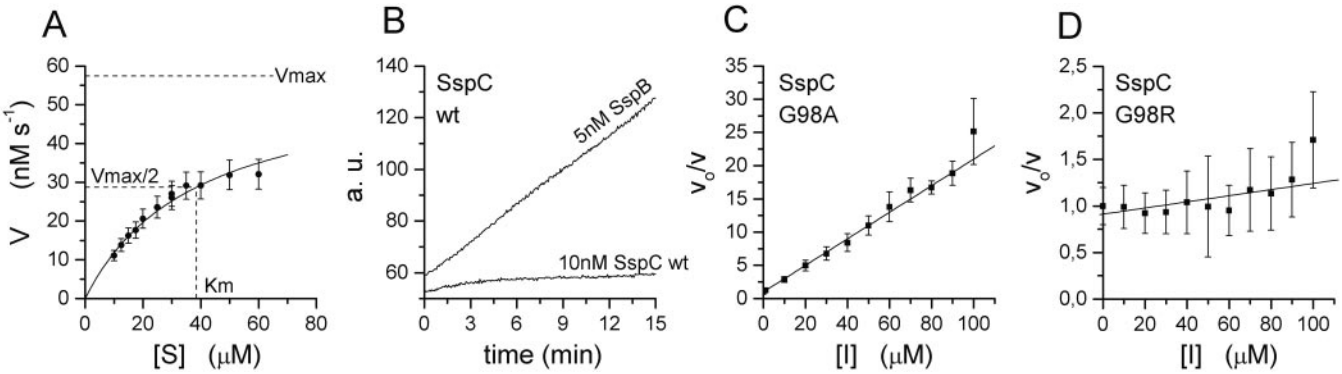

FIG. 5. **Determination of dissociation constants.** *A*, K_m determination for the synthetic substrate Abz-Gln-Gly-Ile-Gly-Thr-Ser-Arg-Pro-Lys(Dnp)-Asp-OH. Assays were performed with 50 nM staphopain B and 10–60 μM substrate. The observed initial velocities were fitted to the Michaelis-Menten equation by hyperbolic regression analysis. *B*, progress curves for substrate hydrolysis by 5 nM staphopain B in the absence and presence of 10 nM wild-type staphostatin B (*SspC wt*). *C*, K_i estimate for the staphostatin B G98A mutant (*SspC G98A*). Assays were performed with a concentration of 100 nM staphopain B and 1 μM substrate. *D*, K_i estimate for the staphostatin B G98R mutant (*SspC G98R*). Assays were performed with a concentration of 50 nM staphopain B and 1 μM substrate.

with a mass of 11,761, matching the molecular mass of the N-terminal processing fragment to within 2 Da (see Fig. 6*B*). Further incubation of mutant inhibitor with protease for 3 h leads to complete degradation of the mutant inhibitor. A similar conversion of the inhibitor into a substrate is observed for the more disruptive glycine to arginine mutation in the P1 position. Again, we observe a processing fragment of the correct molecular weight, and as expected for substrate, the amount of processed fragment grows with the time of incubation (see Fig. 6*C*). Although the arginine mutant is a less efficient substrate for protease than the alanine variant (see Fig. 6*C*), both mutants are more efficiently processed than the wild-type inhibitor, for which the processed fragment is barely detectable in our setup (compare the *three panels* in Fig. 6).

As in the case of the minor processing of wild-type inhibitor, we repeated the experiment with protease from native and recombinant sources to exclude the effect of contaminating proteases. In particular, we can exclude the effect of V8, a protease that is present in culture supernatants of *S. aureus* and was also used for *in vitro* processing of recombinant prostaphopain B to the mature enzyme. Although large amounts of V8 protease (stoichiometric ratio 1:1 and more) can degrade staphostatin B, no degradation fragment corresponding to the molecular weight of the mature staphostatin B can be observed in MALDI-TOF, consistent with the strict preference of V8 for cleavage after glutamic or aspartic acid residues (36).

DISCUSSION

Could the Structure of the Staphopain-Staphostatin Complex Have Been Predicted?—At the outset of this work, experimental structures for staphopain A (21) and staphostatin B (22) were available. With 47% sequence identity between staphopain A and staphopain B, a homology model for staphopain B could be built with reasonable confidence.

Nevertheless, standard three-dimensional dock protocols to dock staphostatin B to the homology model of staphopain B failed to identify the crystallographic complex. In retrospect, this is easy to understand. Superposition of mature staphopain A on the staphopain B model in the complex leads to significant protease-inhibitor overlap. In the absence of a structure of free staphopain B, we cannot distinguish whether the backbone differences between free staphopain A and staphopain B in the complex are because of differences in the structure of the two proteins, or whether they represent structural adaptations of staphopain B on inhibitor binding.

In retrospect, a different computational strategy to identify the binding mode between staphopain B and staphostatin B would have been more successful. In the course of structure verification checks with VERIFY-3D (37, 38) we noted that the binding loop upstream of the most C-terminal β-strand scores very poorly for free inhibitor. In contrast, the very same strand gets excellent scores in the staphopain-staphostatin complex (data not shown). We plan to test on a larger sample of ligand-

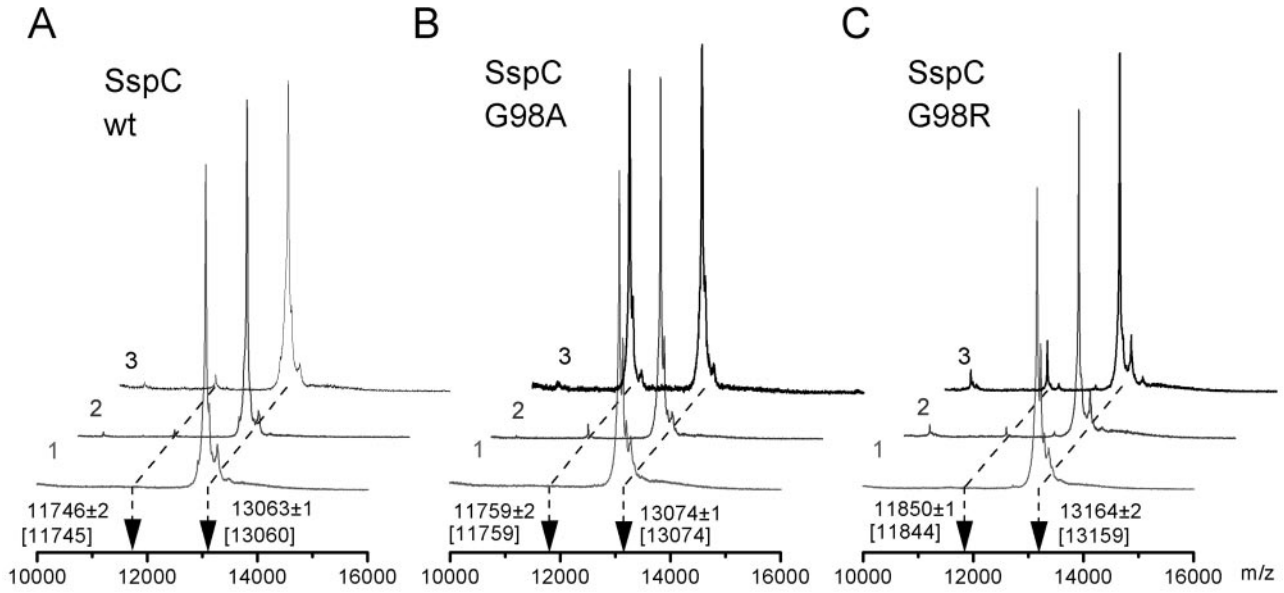

FIG. 6. **MALDI-TOF traces for wild-type (*wt*) staphostatin B and its mutants taken without incubation with protease (*1*, *light gray*), after 5 min of incubation with protease (*2*, *dark gray*), and after 30 min of incubation with protease (*3*, *black trace*).** The major peak in all traces is unprocessed inhibitor, and the smaller peak that grows with time is the N-terminal cleavage fragment. *Below* the peaks, the average mass for the three time points is indicated, with the theoretical value in *brackets* for comparison. Note that the C-terminal fragment is far too light to show up in the displayed mass range, and protease is too heavy.

receptor complexes whether this observation is accidental or whether it applies on a wider scale and could be used for the prediction of ligand-receptor binding modes. For the time being, we caution that the termini of proteins often score poorly in VERIFY3D, and that the method would have also suggested two false positive regions in staphostatin B, the N terminus, and the only helix in the molecule.

A Novel Mechanistic Strategy for Protease Inhibition—Several mechanistic strategies for protease inhibition have emerged from the study of complexes of papain-like cysteine proteases with their inhibitors: cystatins avoid cleavage by meandering around the active site (see Fig. 2*B*); profragments of papain-like proteases span the active site in opposite directions as natural substrates; the same is true of the inhibitors of apoptosis that target caspases (39); in SpeB, the profragment distorts the active site (40); this is also seen in a serine protease-serpin complex (41) and is likely to carry over to complexes of cysteine proteases with serpins; finally distortion of the active site and covalent inhibition have been reported for the complex of p35 with caspase-8 (42). None of these paradigms fits the staphopain-staphostatin complex. Perhaps the closest analogy to our work is found in standard mechanism inhibitors of serine proteases (43). These inhibitors remain soluble, intact molecules after cleavage, held together through extensive contacts between the cleaved parts that are often reinforced through disulfide bridges. Unfortunately, we could not determine whether cleaved staphostatin B is soluble or inhibitory. The limited supply of wild-type protease precluded preparative staphostatin B cleavage, and attempts to produce cleavage products separately failed because the large N-terminal portion of the inhibitor could not be expressed in soluble form.

A Comparison of Binding Modes for Staphostatin B and Substrates—A full understanding of the staphopain-staphostatin complex should explain why staphostatins behave as inhibitors and not as substrates. A comparison of the staphostatin B-staphopain B binding mode with the postulated binding mode (29) of substrates to papain-like proteases is instructive. For substrates, the P2 residue should insert into the S2 pocket and form two main chain hydrogen bonds with protease, as observed for staphostatin B (see Fig. 3). The NH of the P1 glycine should donate a hydrogen bond to Gly-339O, again as observed for staphostatin B. Modeling studies of a papain-substrate complex before nucleophilic attack (44) suggest that the carbonyl oxygen of the scissile peptide bond should point toward Cys-243NH and Gln-237NϵH (in staphopain B numbering), the two residues that according to most authors (29, 44) form the oxyanion hole in papain-like proteases. Our results for the staphostatin B-staphopain B complex are incompatible with this model. As shown in Fig. 3*B*, the unusual main chain conformation of the P1 residue places the P1 carbonyl oxygen far away from its expected location for substrates, so that both nucleophilic attack and stabilization of the tetrahedral intermediate should be compromised, implying a block of the reaction early in the mechanistic cycle.

A Block Early or Late in the Mechanistic Cycle?—Consistent with the structural results, our biochemical data also suggest an early block of the proteolysis reaction. If a tetrahedral intermediate was indeed formed, it should be detectable on denaturing SDS gels, or, because the thioester linkage could be unstable in reducing conditions, especially after boiling of samples in loading buffer, it should manifest itself as two bands with molecular weights corresponding to the free protease and cleaved inhibitor. This was never observed, neither with wild-type nor with recombinant protease preparations. Consistent with the failure to observe a thioester intermediate, we were not able to increase the yield of processed staphostatin B with the addition of hydroxylamine, a common reagent to cleave thioester linkages (data not shown).

The superposition of free and bound inhibitor structures shows that the critical conformation of the P1 glycine of inhibitor is not preformed in the inhibitor structure and results from binding of inhibitor to protease. Our observation that some inhibitor molecules are cleaved immediately on mixing points to imperfections in this process. Once the proper complex is formed, the inhibitor is resistant to cleavage, consistent with no further proteolysis of inhibitor after the initial mixing phase in our experiments.

Interestingly, the peptide Abz-Gln-Gly-Ile-Gly-Thr-Ser-Arg-Pro-Lys(Dnp)-Asp-OH that was designed as a mimic of the binding loop of inhibitor behaves as a slow substrate. There-

fore, it is likely that in the wild-type protease-inhibitor complex, interactions of the binding loop with other parts of the inhibitor in addition to contacts with protease are required for the inhibitory binding mode.

Clearly, more work will be required to elucidate the details of staphostatin-mediated inhibition of staphopains. Nevertheless, it is already clear that the staphopain B-staphostatin B complex shows a new way for a proteinacious inhibitor to inhibit a papain-like cysteine protease. Three key features of this new mode of inhibition stand out: the unusual conformation of the conserved P1 glycine of inhibitor, interactions of the binding loop of inhibitor with both primed and non-primed subsites of protease, and orientation of the binding loop polypeptide chain as in substrates rather than opposite to it as usual in cysteine protease inhibitor complexes. It remains to be seen whether these features characterize a mechanistic outlier among cysteine protease inhibitors, or whether they represent the first example of a more widespread, new "style" of cysteine protease inhibition.

Acknowledgments—We are grateful to Hans Bartunik for generous allocation of beamtime on BW6/DESY, Hamburg, and to Gleb Bourenkov and Galina Kachalova for assistance during data collection. We thank Jerzy Silberring for access to the mass spectrometry facilities at the Mass Spectometry Laboratory, Faculty of Chemistry, Jagiellonian University, Poland, and Tomasz Dylag and Piotr Suder for help with the MS analysis. We are also grateful to Jacek Oledzki and Aleksandra Wyslouch-Cieszynska for mass spectrometry analysis of the substrate cleavage reaction. Grzegorz Dubin shared his staphopain B preparation for comparison with ours. We are grateful to the members of the Warsaw structural biology group, in particular Izabela Sabala and Roman Szczepanowski, for critical reading of the manuscript. Janusz Bujnicki's local structure verification tools were helpful to assess the quality of the structures. Access to the Interdisciplinary Center for Mathematical and Computer Modeling Facilities is gratefully acknowledged.

REFERENCES

1. Hiramatsu, K., Cui, L., Kuroda, M., and Ito, T. (2001) *Trends Microbiol.* **9,** 486–493
2. Hiramatsu, K., Okuma, K., Ma, X. X., Yamamoto, M., Hori, S., and Kapi, M. (2002) *Curr. Opin. Infect. Dis.* **15,** 407–413
3. Pearson, H. (2002) *Nature* **418,** 469
4. Maskalyk, J. (2002) *Can. Med. Assoc. J.* **167,** 375
5. Goldstein, E. J., Citron, D. M., Merriam, C. V., Warren, Y. A., Tyrrell, K. L., and Fernandez, H. T. (2003) *Antimicrob. Agents Chemother.* **47,** 337–341
6. Viale, P., Scolari, C., Colombini, P., Cristini, F., Cadeo, B., and Pagani, L. (2002) *J. Chemother.* **14,** 526–529
7. Moise, P. A., Forrest, A., Birmingham, M. C., and Schentag, J. J. (2002) *J. Antimicrob. Chemother.* **50,** 1017–1026
8. Delgado, G., Jr., Neuhauser, M. M., Bearden, D. T., and Danziger, L. H. (2000) *Pharmacotherapy* **20,** 1469–1485
9. Evans, G. A. (2002) *Curr. Infect. Dis. Rep.* **4,** 17–27
10. Bailey, C. J., Lockhart, B. P., Redpath, M. B., and Smith, T. P. (1995) *Med. Microbiol. Immunol.* **184,** 53–61
11. Gemmell, C. G. (1995) *J. Med. Microbiol.* **43,** 318–327
12. Lee, L. Y., Miyamoto, Y. J., McIntyre, B. W., Hook, M., McCrea, K. W., McDevitt, D., and Brown, E. L. (2002) *J. Clin. Invest.* **110,** 1461–1471
13. Palma, M., Haggar, A., and Flock, J. I. (1999) *J. Bacteriol.* **181,** 2840–2845
14. Ji, G., Beavis, R. C., and Novick, R. P. (1995) *Proc. Natl. Acad. Sci. U. S. A.* **92,** 12055–12059
15. Mayville, P., Ji, G., Beavis, R., Yang, H., Goger, M., Novick, R. P., and Muir, T. W. (1999) *Proc. Natl. Acad. Sci. U. S. A.* **96,** 1218–1223
16. Travis, J., Potempa, J., and Maeda, H. (1995) *Trends Microbiol.* **3,** 405–407
17. Coulter, S. N., Schwan, W. R., Ng, E. Y., Langhorne, M. H., Ritchie, H. D., Westbrock-Wadman, S., Hufnagle, W. O., Folger, K. R., Bayer, A. S., and Stover, C. K. (1998) *Mol. Microbiol.* **30,** 393–404
18. Rice, K., Peralta, R., Bast, D., de Azavedo, J., and McGavin, M. J. (2001) *Infect. Immun.* **69,** 159–169
19. Massimi, I., Park, E., Rice, K., Müller-Esterl, W., Sauder, D., and McGavin, M. J. (2002) *J. Biol. Chem.* **277,** 41770–41777
20. Rzychon, M., Sabat, A., Kosowska, K., Potempa, J., and Dubin, A. (2003) *Mol. Microbiol.* **49,** 1051–1066
21. Hofmann, B., Schomburg, D., and Hecht, H. J. (1993) *Acta Crystallogr.* **49,** (suppl.) 102–102
22. Rzychon, M., Filipek, R., Sabat, A., Kosowska, K., Dubin, A., Potempa, J., and Bochtler, M. (2003) *Protein Sci.* **12,** in press
23. Chavira, R., Jr., Burnett, T. J., and Hageman, J. H. (1984) *Anal. Biochem.* **136,** 446–450
24. Berthold, H., Frorath, B., Scanarini, M., Abney, C. C., Ernst, B., and Northemann, W. (1992) *Biotech. Lett.* **14,** 245–250
25. Bower, M. J., Cohen, F. E., and Dunbrack, R. L., Jr. (1997) *J. Mol. Biol.* **267,** 1268–1282
26. Vagin, A., and Teplyakov, A. (1997) *J. Appl. Crystallogr.* **30,** 1022–1025
27. Cowtan, K. (1998) *Acta Crystallogr. Sect. D Biol. Crystallogr.* **54**, 750–756
28. Perrakis, A., Morris, R., and Lamzin, V. S. (1999) *Nat. Struct. Biol.* **6,** 458–463
29. McGrath, M. E. (1999) *Annu. Rev. Biophys. Biomol. Struct.* **28,** 181–204
30. Stubbs, M. T., Laber, B., Bode, W., Huber, R., Jerala, R., Lenarcic, B., and Turk, V. (1990) *EMBO J.* **9,** 1939–1947
31. Coulombe, R., Grochulski, P., Sivaraman, J., Menard, R., Mort, J. S., and Cygler, M. (1996) *EMBO J.* **15,** 5492–5503
32. Cygler, M., Sivaraman, J., Grochulski, P., Coulombe, R., Storer, A. C., and Mort, J. S. (1996) *Structure* **4,** 405–416
33. Schechter, I., and Berger, A. (1967) *Biochem. Biophys. Res. Commun.* **27,** 157–162
34. Lewis, S. D., Johnson, F. A., and Shafer, J. A. (1976) *Biochemistry* **15,** 5009–5017
35. Bürgi, H. B., Dunitz, J. D., and Shefter, E. (1973) *J. Am. Chem. Soc.* **95,** 5065–5067
36. Vasseur, C., Galacteros, F., Groff, P., and Wajcman, H. (1991) *J. Biochem. Biophys. Methods* **22,** 195–205
37. Eisenberg, D., Luthy, R., and Bowie, J. U. (1997) *Methods Enzymol.* **277,** 396–404
38. Bowie, J. U., Luthy, R., and Eisenberg, D. (1991) *Science* **253,** 164–170
39. Stennicke, H. R., Ryan, C. A., and Salvesen, G. S. (2002) *Trends Biochem. Sci* **27,** 94–101
40. Kagawa, T. F., Cooney, J. C., Baker, H. M., McSweeney, S., Liu, M., Gubba, S., Musser, J. M., and Baker, E. N. (2000) *Proc. Natl. Acad. Sci. U. S. A.* **97,** 2235–2240
41. Huntington, J. A., Read, R. J., and Carrell, R. W. (2000) *Nature* **407,** 923–926
42. Xu, G., Cirilli, M., Huang, Y., Rich, R. L., Myszka, D. G., and Wu, H. (2001) *Nature* **410,** 494–497
43. Bode, W., and Huber, R. (1992) *Eur. J. Biochem.* **204,** 433–451
44. Harrison, M. J., Burton, N. A., and Hillier, I. H. (1997) *J. Am. Chem. Soc.* **119,** 12285–12291